

Optical Properties of the Rhodotron Bending Magnets *

O. Gal^{a†}, J.-M. Capdevila^a, A. Nguyen^a, Y. Jongen^b, M. Abs^b, F. Genin^b
^a CEA-LETI-DEIN – Centre d'Études de Saclay – 91191 Gif-sur-Yvette – France
^b I.B.A. s.a. – Chemin du Cyclotron, 2 – 1348 Louvain-la-Neuve – Belgium

Abstract

We present a general analytical derivation of the fringing-field effects in a 2D static magnetic field with median-plane symmetry. We obtain the corresponding matrix coefficients expanded in powers of the gap-over-gyroradius ratio and shape integrals of the field profile. Comparison is made with direct ray-tracing calculations for the case of the Rhodotron bending magnets, where this ratio is very large.

1. INTRODUCTION

For compactness reasons, the bending magnets of the 10 MeV, 100 kW Rhodotron [1-3,7] exhibit a very large gap-over-gyroradius ratio ($g/R_0 = 0.3$ to 0.45). This leads to important fringing-field effects (shifted effective trajectory, predominant correction in the effective incidence angle for the vertical focusing). In the literature these effects, when handled, are calculated to first order in g/R_0 [4,5]. It is thus pertinent to ask whether these results are still valid in the case of the Rhodotron magnets. Astonishingly, the answer is rather positive but the formulation is singularly complicated.

2. MOTION IN A 2D STATIC MAGNETIC FIELD WITH MEDIAN-PLANE SYMMETRY

2.1. Equations of motion

We start with the equations of motion for charged particles, of charge q , in a static magnetic field which is constant in the X direction and possesses a median-plane symmetry relative to $Y=0$. The components of the field are thus, expanded to second order in Y :

$$\begin{aligned} B_x(Y,Z) &= 0 & B_z(Y,Z) &= Y \cdot B'(Z) + o(Y^2) \\ B_y(Y,Z) &= B(Z) - \frac{1}{2} Y^2 \cdot B''(Z) + o(Y^2), \end{aligned} \quad (1)$$

where $B(Z)$ is the only component, B_y , of the field in the median plane and the prime denotes the derivative with respect to Z . The equations may be obtained in the form:

$$\begin{aligned} dX/dZ &= \tan \varphi & dY/dZ &= \tan \eta / \cos \varphi \\ dL/dZ &= 1 / (\cos \varphi \cdot \cos \eta) \\ \frac{d\varphi}{dZ} &= -\frac{1}{R_0(1+\delta)} \frac{1}{\cos \eta} \left[\frac{1}{\cos \varphi} \frac{B_y}{B_0} - \tan \eta \frac{B_z}{B_0} \right] \\ \frac{d\eta}{dZ} &= -\frac{1}{R_0(1+\delta)} \frac{\tan \varphi}{\cos \eta} \frac{B_z}{B_0}, \end{aligned} \quad (2)$$

where δ is the momentum deviation:

$$\delta = (p - p_0) / p_0, \quad (3)$$

and φ and η are the momentum azimuth in the (Z, X) plane and inclination to that plane (see Fig. 1). The

components of momentum \mathbf{p} are thus:

$$\begin{aligned} p_x &= p \cdot \cos \eta \cdot \sin \varphi \\ p_y &= p \cdot \sin \eta \\ p_z &= p \cdot \cos \eta \cdot \cos \varphi. \end{aligned} \quad (4)$$

In Eqs. (2), B_0 is a value of reference for the magnetic field, which in the following sections will be the constant value of the B_y component

far inside the dipole magnet. By convention, the Y axis is taken such that $qB_0 > 0$. A reference momentum, p_0 , is also defined, corresponding to the reference gyroradius:

$$R_0 = p_0 / qB_0. \quad (5)$$

Note that Z has been taken as the independent variable and time has been replaced by the length traversed, L .

In the following, we shall suppose that the profile goes from zero to a constant equal to B_0 through a finite length:

$$\begin{aligned} B(Z \leq Z^A) &= 0 \\ B(Z \geq Z^B) &= B_0 \end{aligned} \quad (6)$$

(see Fig. 2). In the fixed reference system (X, Y, Z) , fringing-field effects can be completely calculated and expanded in terms of pure shape integrals of the field profile

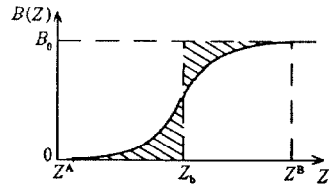


Figure 2 : Fringing field of finite extension, with field boundary at Z_b .

2.2. Trajectories in median plane

Since B_y is the only component of the field in the median plane $Y=0$, trajectories with $Y=\eta=0$ exist. The equation of motion (2) for φ gives then [4]:

$$\sin \varphi(Z) = \sin \varphi^A - (g/R_0) K(Z) / (1+\delta), \quad (7)$$

where $K(Z)$ is the integral of the field profile:

$$K(Z) = \int_{Z^A}^Z \frac{B(Z)}{B_0} \frac{dZ}{g} = \int_{-\infty}^Z \frac{B(Z)}{B_0} \frac{dZ}{g}, \quad (8)$$

normalized with B_0 and the length g , characteristic of the field gradient. Usually, g is the air gap of the magnet.

It is obvious that we obtain the same angle φ^B at Z^B (or at any farther position) if we replace the profile $B(Z)$ by a step profile starting at the plane $Z = Z_b$, called the *equivalent field boundary* and given by [4]:

$$Z_b = Z_r - g \cdot I_0, \quad I_0 = \int_{-\infty}^{+\infty} \left[\frac{B(Z)}{B_0} - \mathcal{K}(Z - Z_r) \right] \frac{dZ}{g} \quad (9)$$

(see Fig. 2). The function $\mathcal{K}(Z)$ is the unit step and Z_r is, for example, the mechanical magnet boundary position (or any other reference position). This field boundary does not depend on gyroradius $R_0(1+\delta)$ nor on initial angle φ^A , and

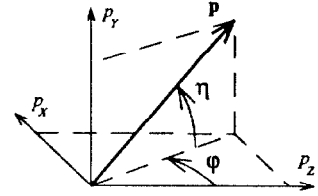


Figure 1 : Angular variables for the momentum.

* Collaboration C.E.A.-I.B.A. † Corresponding author.

defines the *equivalent, uniform magnet*.

Using the Taylor developments of $\tan\varphi$ and $1/\cos\varphi$ in $\sin\varphi$ and denoting the corresponding coefficients by:

$$\alpha_n(\varphi) = \frac{1}{n!} \frac{d^n \tan\varphi}{d(\sin\varphi)^n}, \quad \beta_n(\varphi) = \frac{1}{n!} \frac{d^n (1/\cos\varphi)}{d(\sin\varphi)^n}, \quad (10)$$

we can integrate the equations of motion (2) for X and L . Comparing the values X^B and L^B at Z^B with those given by the equivalent magnet shows that the equivalent trajectory must undergo a shift ΔX in X (see Fig. 3) and ΔL in L , given by:

$$\begin{aligned} \frac{\Delta X}{R_0} &= \sum_{n=1}^{\infty} (-1)^n (g/R_0)^{n+1} (1+\delta)^{-n} \alpha_n(\varphi^A) I_n \\ \frac{\Delta L}{R_0} &= \sum_{n=1}^{\infty} (-1)^n (g/R_0)^{n+1} (1+\delta)^{-n} \beta_n(\varphi^A) I_n \\ I_n &= \int_{-\infty}^{+\infty} [K^n(Z) - K^{*n}(Z)] \frac{dZ}{g} \quad (n \geq 1), \end{aligned} \quad (11)$$

where $K^*(Z)$ denotes the integral (8) obtained for the equivalent step profile. These shifts are zero for a step profile and are due to the fringing-field finite extension. The integrals I_n are shape factors characterizing the field profile $B(Z)/B_0$.

2.3. Trajectories out of median plane

When dealing with trajectories not restricted to the median plane, it is necessary to resort to a limited development in Y and η , taken here to second order. The natural form for the results is an expansion in powers of g/R_0 when considering the following normalized variables:

$$\hat{X} = X/R_0, \quad \hat{Y} = Y/R_0, \quad \hat{L} = L/R_0, \quad \hat{Z} = Z/g. \quad (12)$$

Because they are odd in Y, η , the equations of motion (2) for Y and η are of first order here and the zero-order expression (7) for $\varphi(Z)$ is thus sufficient. The solution of the linear system of these two equations may be written

$$\begin{aligned} \hat{Y}(\hat{Z}) &= C(\hat{Z}) \cdot \hat{Y}^A + S(\hat{Z}) \cdot \eta^A \\ \eta(\hat{Z}) &= C'(\hat{Z}) \cdot \hat{Y}^A + S'(\hat{Z}) \cdot \eta^A \end{aligned} \quad (13)$$

where $C'(\hat{Z}), S'(\hat{Z})$ are not the derivatives of $C(\hat{Z}), S(\hat{Z})$. Taking the g/R_0 expansion of these functions in the form

$$f(\hat{Z}, g/R_0) = \sum_{n=0}^{\infty} (g/R_0)^n \cdot f_{(n)}(\hat{Z}), \quad (14)$$

we obtain:

$$\begin{aligned} C_{(n)}(\hat{Z}) &= \sum_{k=0}^{n-1} (-1)^k \frac{\beta_k(\varphi^A)}{(1+\delta)^k} \int_{\hat{Z}^A}^{\hat{Z}} K^k \cdot C'_{(n-k-1)} d\hat{Z} \quad [+1 \text{ if } n=0] \\ S_{(n)}(\hat{Z}) &= \sum_{k=0}^{n-1} (-1)^k \frac{\beta_k(\varphi^A)}{(1+\delta)^k} \int_{\hat{Z}^A}^{\hat{Z}} K^k \cdot S'_{(n-k-1)} d\hat{Z} \\ C'_{(n)}(\hat{Z}) &= -\sum_{k=0}^n (-1)^k \frac{\alpha_k(\varphi^A)}{(1+\delta)^{k+1}} \int_{\hat{Z}^A}^{\hat{Z}} K^k \cdot C_{(n-k)} \cdot \hat{B}' d\hat{Z} \end{aligned} \quad (15)$$

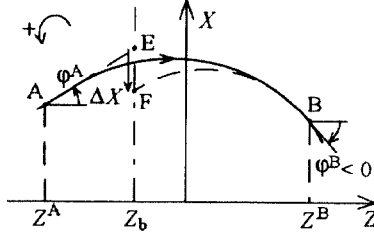


Figure 3 : Real trajectory (—) and shifted equivalent trajectory (---) in median plane.

$$S'_{(n)}(\hat{Z}) = -\sum_{k=0}^n (-1)^k \frac{\alpha_k(\varphi^A)}{(1+\delta)^{k+1}} \int_{\hat{Z}^A}^{\hat{Z}} K^k \cdot S_{(n-k)} \cdot \hat{B}' d\hat{Z} \quad [+1 \text{ if } n=0]$$

where $\hat{B}(\hat{Z}) = B(Z)/B_0$ and $\hat{B}'(\hat{Z}) = d\hat{B}/d\hat{Z}$. This recurrent system gives every function $C_{(n)}, S_{(n)}, C'_{(n)}, S'_{(n)}$ at any order n but calculations are rapidly very complicated (see Sec. 3).

The equations of motion (2) for \hat{X}, φ and \hat{L} are even in \hat{Y}, η and the part of zero order, denoted here by $\hat{X}_h(\hat{Z}), \varphi_h(\hat{Z})$ and $\hat{L}_h(\hat{Z})$ (h for "horizontal"), has been already calculated in Section 2.2. We may then derive evolution equations for the second-order part, denoted by $\hat{X}_v(\hat{Z}), \varphi_v(\hat{Z}), \hat{L}_v(\hat{Z})$ (v for "vertical"), with the initial values $\hat{X}_v^A = \varphi_v^A = \hat{L}_v^A = 0$. The solution may be written

$$\begin{aligned} \hat{X}_v(\hat{Z}) &= F_1(\hat{Z}) \cdot \hat{Y}^{A^2} + F_2(\hat{Z}) \cdot \hat{Y}^A \eta^A + F_3(\hat{Z}) \cdot \eta^{A^2} \\ \varphi_v(\hat{Z}) &= G_1(\hat{Z}) \cdot \hat{Y}^{A^2} + G_2(\hat{Z}) \cdot \hat{Y}^A \eta^A + G_3(\hat{Z}) \cdot \eta^{A^2} \\ \hat{L}_v(\hat{Z}) &= H_1(\hat{Z}) \cdot \hat{Y}^{A^2} + H_2(\hat{Z}) \cdot \hat{Y}^A \eta^A + H_3(\hat{Z}) \cdot \eta^{A^2}, \end{aligned} \quad (16)$$

and a chain of equations on the functions $F_{i(n)}, G_{i(n)}, H_{i(n)}$, such as Eqs. (15), may be obtained. It is interesting to note that, due to a term $\frac{1}{2}(R_0/g)\hat{B}''\hat{Y}^2/\cos\varphi^A$ in $d\varphi_v/d\hat{Z}$, the coefficient $G_{1(-1)}$ is non-zero, but only in the region where the field gradient is non-zero. This singularity leads to the well-known second-order shift in X for $g/R_0 \rightarrow 0$.

The fringing-field effects are properly described by the transformation $E \rightarrow F$, where E is the image of A by a drift up to the field boundary and F is the reciprocal image of B by the equivalent magnet (see Fig. 3). Expanded coefficients for this transformation may be derived from those of the $A \rightarrow B$ transformation.

3. TRANSPORT COEFFICIENTS FOR THE FRINGING-FIELD EFFECTS

The transport matrices will be expressed in a *paraxial phase-space* relative to the *reference trajectory*. This trajectory, restrained in the median plane, is obtained for the momentum p_0 and the initial incidence $\varphi^A = i_0$.

Each point M_0 on this trajectory defines a local reference system (M_0, x, y, z) with z tangent to the reference trajectory, and $y = Y$, from where x is in the local centrifugal direction (see Fig. 4). We also define ε as the inclination of trajectory projection on median plane to z axis, or:

$$p_x/p_0 = (1+\delta) \cdot \sin\varepsilon \cdot \cos\eta. \quad (17)$$

Motion is thus described in a non-dimensional paraxial phase-space $(x_i)_{1 \leq i \leq 6}$ with:

$$\begin{aligned} x_1 = \hat{x} = x/R_0 & \quad x_2 = \varepsilon & \quad x_3 = \hat{y} = y/R_0 & \quad x_4 = \eta \\ x_5 = \lambda = (L - L_0)/R_0 & & \quad x_6 = \delta. \end{aligned} \quad (18)$$

Note that this phase-space is not *symplectic* (Liouville theorem is not applicable) excepted to first order.

Transformation from a plane A to a plane B is expressed

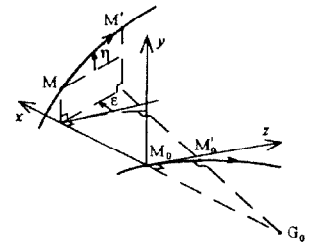


Figure 4 : Paraxial-variable definition. Point M_0 is on the reference trajectory.

to second order in paraxial variables in the usual form [5]:

$$x_i^B = \sum_{1 \leq j \leq 6} (x_i^B | x_j^A) x_j^A + \sum_{1 \leq j \leq k \leq 6} (x_i^B | x_j^A x_k^A) x_j^A x_k^A \quad (19)$$

where $(x_i^B | x_j^A)$ and $(x_i^B | x_j^A x_k^A)$ denote first- and second-order coefficients of the transformation.

In the case of E \rightarrow F transformation defined in Sec. 2, the coefficients are obtained by expressing the x_i 's in terms of X, L, φ, δ at E and F and expanding them to second order in the paraxial variables. We thus obtain, to second order in g/R_0 (we limit ourself to first-order coefficients here):

$$\begin{aligned} (\hat{x}^F | \hat{x}^E) &= (\epsilon^F | \epsilon^E) = (\lambda^F | \lambda^E) = (\delta^F | \delta^E) = 1 \quad (20) \\ (\hat{x}^F | \epsilon^E) &= -3 \left(\frac{g}{R_0} \right)^2 \frac{\sin i_0}{\cos^3 i_0} I_1 \quad (\hat{x}^F | \delta^E) = \left(\frac{g}{R_0} \right)^2 \frac{1}{\cos^2 i_0} I_1 \\ (\lambda^F | \epsilon^E) &= - \left(\frac{g}{R_0} \right)^2 \frac{1 + 2 \sin^2 i_0}{\cos^4 i_0} I_1 \quad (\lambda^F | \delta^E) = \left(\frac{g}{R_0} \right)^2 \frac{\sin i_0}{\cos^3 i_0} I_1 \\ (\hat{y}^F | \hat{y}^E) &= 1 - \left(\frac{g}{R_0} \right)^2 \frac{1 + \sin^2 i_0}{\cos^4 i_0} J_{1,2} \quad (\hat{y}^F | \eta^E) = \left(\frac{g}{R_0} \right)^2 \frac{\sin i_0}{\cos^3 i_0} J_{1,1} \\ (\eta^F | \hat{y}^E) &= -\tan i_0 + \frac{g}{R_0} \frac{1 + \sin^2 i_0}{\cos^3 i_0} J_{0,2} \\ &+ \left(\frac{g}{R_0} \right)^2 \left[\frac{\sin i_0 (1 + \sin^2 i_0)}{\cos^5 i_0} J_{1,2} - \frac{\sin i_0 (7 + 3 \sin^2 i_0)}{\cos^5 i_0} J_{0,2,1} \right] \\ (\eta^F | \eta^E) &= 1 + \left(\frac{g}{R_0} \right)^2 \left[\frac{1 + \sin^2 i_0}{\cos^4 i_0} J_{1,2} - \frac{\sin^2 i_0}{\cos^4 i_0} J_{1,1} \right], \end{aligned}$$

where I_1 is given by Eq. (11c), and other shape factors are:

$$J_{n,p,q} = \int_{-\infty}^{+\infty} (\hat{Z} - \hat{Z}_b)^n \cdot \left[\hat{B}^{*p} K^{*q} - \hat{B}^p K^q \right] d\hat{Z} \quad (21)$$

Because of alternate parity of the trigonometric polynomial, with $\sin i_0$ small, second-order term may be of the same order of magnitude as the third-order one, which yields then poor precision at that order. Note that determinant is 1.

4. APPLICATION TO THE RHODOTRON BENDING MAGNETS

The *Rhodotron TT-200*[®] industrial machine constructed by I.B.A. is a 10 MeV, 10 passes, 100 kW continuous electron accelerator [2,3,7]. There are 9 bending magnets with 194°, 8×198° deflection angles and 125 mm, 8×170 mm gyration radii. Magnet faces with proper inclination angle i_0 is the only focusing device interposed along the 27 m acceleration path. Magnet air gap is 55 mm, which gives $g/R_0=0.44$ for the first

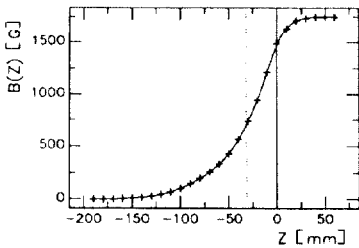


Figure 5 : Field profile measured in Rhodotron bending magnets.

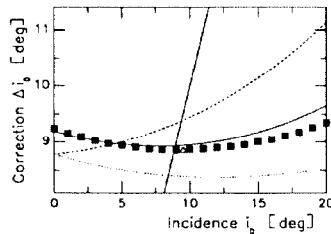


Figure 6 : Comparison between analytical evaluations (— 1st order, 2nd order, — 3rd order in g/R_0) of correction Δi_0 and direct ray-tracing evaluation (■) for $g/R_0=0.44$ (Δ : Rhodotron first-bending magnet).

bending and $g/R_0=0.32$ for the others.

The field profile measured on the machine is represented in Fig. 5, with a cubic spline interpolation necessary for the second-order trajectory calculations. Table 1 gives the shape integrals obtained for that interpolating profile with, for comparison, those obtained for a linear ramp of length $2g$.

The most important fringing-field effect is the modification of coefficient $(\eta^F | \hat{y}^E)$, which may be written

$$(\eta^F | \hat{y}^E) = -\tan(i_0 - \Delta i_0), \quad (22)$$

where Δi_0 is a correction given by Eqs. (20). Its first-order part in g/R_0 is well known [4,5] but in our case, it was crucial to know it with a precision better than 0.5°. As it may be seen from Fig. 6, the aimed precision is obtained to third-order. The correction is resp. 8.9° and 6.5° for the first and following bendings ($i_0 = 9.5^\circ$ and 7.5°)

5. CONCLUSION

We have presented an analytical derivation of fringing-field effects in bending magnets expanded in powers of g/R_0 and pure shape integrals of the field profile. At first order we recover the well-known Δi_0 correction in $(\eta^F | \hat{y}^E)$ coefficient. We give also original higher-order expressions, which for example are not in accordance with [5,6], but agree well with direct second-order ray-tracing calculations made in the case of Rhodotron bending magnets. Many important details of the algebra are occulted in this paper, and this topic will be developed in an article to be soon published.

REFERENCES

- [1] J. Pottier, "A new type of RF electron accelerator: the Rhodotron", Nucl. Instr. Meth. Phys. Res., vol. B40/41, pp. 943-945, 1989.
- [2] O. Gal *et al.*, "Numerical and experimental results on the beam dynamics in the Rhodotron accelerator", in Proc. of the Third E.P.A.C., Berlin, Germany, March 1992, vol. 1, pp. 819-821.
- [3] Y. Jongen *et al.*, "The Rhodotron, a 10 MeV, 100 kW beam power metric wave, cw electron accelerator", in Proc. of the 7th All-Union Conf. on Applied Accel., St Petersburg, Russian Fed., 1992.
- [4] H. Wollnik, Optics of Charged Particles, Orlando: Academic Press, 1987.
- [5] K. L. Brown, "A first- and second-order matrix theory for the design of beam transport systems and charged particle spectrometers", Advances Part. Phys., vol. 1, pp. 71-134, 1968. See also TRANSPORT documentation
- [6] B. Hartmann and H. Wollnik, "Third-order particle motion through the fringing field of a homogeneous bending magnet", Nucl. Instr. Meth. Phys. Res., vol. A344, pp. 278-285, 1994.
- [7] M. Abs *et al.*, "First beam test results of the 10 MeV, 100 kW, Rhodotron", in this conference, WEP38W.

Table 1 : Shape factors for the measured field profile and for the linear ramp of length $2g$.

	Measured profile	Linear ramp
I_0	0.573	—
I_1	0.210	$\frac{1}{6} \approx 0.167$
I_2	0.063	$\frac{1}{15} \approx 0.067$
$J_{1,1}$	0.210	$\frac{1}{6} \approx 0.167$
$J_{0,2}$	0.351	$\frac{1}{3} \approx 0.333$
$J_{1,2}$	0.144	$\frac{1}{6} \approx 0.167$
$J_{0,2,1}$	0.093	$\frac{1}{10} = 0.1$